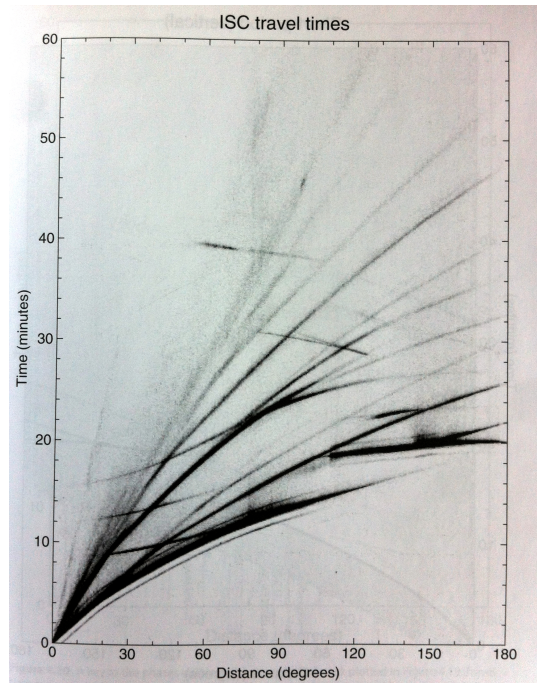


3 Body Waves: Medium & physical approximations, mode-ray duality, seismic phases, traveltimes, Earth structure



Travel-time curves for different earthquake phases measured in the Earth.

Introduction

Body waves are waves that traverse the Earth's subsurface and exist as a solution to the momentum equation in any setting, unlike surface waves which only appear due to a free surface, and free oscillations which only appear if the propagation space is fully enclosed. In this chapter, we shall study the solutions due to simplifying assumptions upon the model space, starting with a homogeneous fullspace (no boundaries or medium changes), and a half space (free surface over a homogeneous domain). Later, we shall abandon these approximations in media complexity but rather approximate the solutions, or physics of wave propagation.

Learn objectives

- You are familiar with Lamé's theorem and Helmholtz potentials to separate P- and S-wave components.
- You know the characteristics of the far-field term of P-waves.
- You are able to explain for what settings analytical solutions can still be found.
- You know what triplication of seismic phases means.
- You are familiar with the nomenclature of seismic phases in the Earth.

3.1 Model-space approximations

As we have seen previously, we can write the inhomogeneous equations of motion as follows: Let \mathbf{u} be a continuous displacement vector in an everywhere solid Earth model \oplus bounded by $\partial\oplus$ and characterized by density ρ and elastic tensor \mathbf{c} . The linearized momentum equation due to an indigenous body-force excitation \mathbf{f} (representing earthquakes) in \oplus reads

$$\rho \partial_t^2 \mathbf{u} - \nabla \cdot \boldsymbol{\tau} = \mathbf{f} \text{ in } \oplus \quad (3.1)$$

subject to the constitutive elastic stress-strain relationship (“Hooke’s Law”)

$$\boldsymbol{\tau} = \mathbf{c} : \nabla \mathbf{u} \text{ in } \oplus, \quad (3.2)$$

and the dynamical free-surface boundary condition

$$\hat{\mathbf{n}} \cdot \boldsymbol{\tau} = \mathbf{0} \text{ on } \partial\oplus. \quad (3.3)$$

Lamé’s Theorem and potentials

We shall further assume isotropic wavespeed variations $\tau_{ij} = \lambda \delta_{ij} \partial_k u_k + \mu \partial_i u_j$, using the Lamé parameters λ and μ to describe the material properties, such that eq. (3.1) can be “simplified” as

$$\rho \partial_t^2 \mathbf{u} - (\lambda + 2\mu) \nabla (\nabla \cdot \mathbf{u}) + \mu \nabla \times (\nabla \times \mathbf{u}) = \mathbf{f} \text{ in } \oplus. \quad (3.4)$$

This form has immediate qualitative ramifications for the solutions \mathbf{u} : The second term on the left hand side contains a divergence on \mathbf{u} , which can be viewed as a volumetric change (recall the divergence theorem), and hints at compressional waves related to elastic parameters $(\lambda + 2\mu)$. The third term contains a double curl on \mathbf{u} which hints at rotating particle motion without volumetric change, i.e. shear waves.

In the following, we will utilize potential theory to work out further simplifications of eq. (3.4).

Lamé’s Theorem. Suppose $\mathbf{u}(\mathbf{x}, t)$ is the unique solution to the momentum equation eq. (3.4). Expressing source term, initial displacement and velocity vectors with Helmholtz potentials

$$\mathbf{f} = \nabla \Phi + \nabla \times \Psi; \quad \dot{\mathbf{u}}(\mathbf{x}, 0) = \nabla A + \nabla \times \mathbf{B}; \quad \mathbf{u}(\mathbf{x}, 0) = \nabla C + \nabla \times \mathbf{D} \quad (3.5)$$

with $\nabla \cdot \Psi = \nabla \cdot \mathbf{B} = \nabla \cdot \mathbf{D} = 0$, there exist potentials ϕ and ψ for \mathbf{u} with all of the four properties:

- | | | |
|---|---|--|
| (i) $\mathbf{u} = \nabla \phi + \nabla \times \psi$ | (iii) $\ddot{\phi} = \frac{\Phi}{\rho} + v_p^2 \nabla^2 \phi$ | (where $\rho v_p^2 = \lambda + 2\mu$) |
| (ii) $\nabla \cdot \psi = 0$ | (iv) $\ddot{\psi} = \frac{\Psi}{\rho} + v_s^2 \nabla^2 \psi$ | (where $\rho v_s^2 = \mu$) |

$\nabla \phi$ and $\nabla \times \psi$ are called the *P-wave* and *S-wave components* of \mathbf{u} , respectively.

Mathematical excursion: Potential theory and vector fields

Helmholtz Theorem. Any vector field \mathbf{u} that is continuous and zero at infinity can be expressed as the gradient of a scalar and the curl of a vector as

$$\mathbf{u} = \nabla\phi + \nabla \times \boldsymbol{\psi}, \quad (3.6)$$

where $\nabla\phi$ and $\nabla \times \boldsymbol{\psi}$ are orthogonal in the integral norm; ϕ is the scalar potential of \mathbf{u} , and $\boldsymbol{\Psi}$ the vector potential (proof e.g. in Blakely, p. 29).

It is sufficient to solve the vector Poisson equation $\nabla^2 \mathbf{W} = \mathbf{u}$, which is given by

$$\mathbf{W}(\mathbf{x}) = \int_{\oplus} \frac{\mathbf{u}(\boldsymbol{\xi})}{4\pi |\mathbf{x} - \boldsymbol{\xi}|} d^3\boldsymbol{\xi}, \quad (3.7)$$

to obtain the potentials via $\phi = \nabla \cdot \mathbf{W}$ and $\boldsymbol{\psi} = -\nabla \times \mathbf{W}$.

Conservative vector fields: If $\phi \neq 0$ then \mathbf{u} is conservative. A vector field is *irrotational* and has no vorticity if its curl vanishes everywhere, i.e. $\nabla \times \mathbf{u} = \mathbf{0}$, and this is a necessary and sufficient condition for the existence of a scalar potential (gravitational attraction *around* a mass body).

Solenoidal vector fields: If $\nabla \cdot \mathbf{u} = 0$, then the field has no “sources” or “sinks” and is purely rotational. This is a necessary and sufficient condition for $\mathbf{u} = \nabla \times \boldsymbol{\psi}$ (e.g. gravitational attraction *between* two mass bodies).

Another useful application of Helmholtz potentials is found in representing a tangent vector field $\mathbf{u}^\Omega = \nabla_1 V - \hat{\mathbf{r}} \times \nabla_1 W$ to circumvent the singularities at the polar axis in spherical coordinates. ∇_1 is the *surface gradient operator* defined via $\nabla = \hat{\mathbf{n}}(\hat{\mathbf{n}} \cdot \nabla) + \nabla_1$ and $\int_\Omega V d\Omega = \int_\Omega W d\Omega = 0$ (see Dahlen & Tromp, p. 868-869).

Lamé’s Proof. Integrate $\ddot{\phi}$ and $\ddot{\boldsymbol{\psi}}$, and verify (i)–(iv). (i) and (ii) are trivial, and (iii) follows upon recognizing $\nabla^2 \phi = \nabla \mathbf{u}$ from (i). (iv) follows similarly using Lagrange’s formula $\nabla^2 \boldsymbol{\psi} = \nabla(\nabla \cdot \boldsymbol{\psi}) - \nabla \times (\nabla \times \boldsymbol{\psi})$ and other vector identities $\nabla \times (\nabla \phi) = \mathbf{0}$ and $\nabla \cdot (\nabla \times \boldsymbol{\psi}) = 0$.

3.2 Analytical solutions

Analytical solution in a homogeneous fullspace

Assuming a unit point source in space and time $\mathbf{f} = \delta(t)\delta(\mathbf{x})\hat{\mathbf{x}}$, we first study the scalar version

$$\partial_t^2 g = \delta(\mathbf{x})\delta(t) + c^2 \nabla^2 g \quad (3.8)$$

with zero initial conditions and c being the wavespeed. This has the simple solution

$$g(\mathbf{x}, t) = \frac{1}{4\pi c^2} \frac{\delta(t - |\mathbf{x}|/c)}{|\mathbf{x}|}, \quad (3.9)$$

which has three major properties:

- Spatial dependence is controlled by the product of a rapidly fluctuating function δ and a slowly varying function $1/|\mathbf{x}|$.
- The rapidly varying function depends only on time t relative to *arrival time* $|\mathbf{x}|/c$.
- The wave shape at any distance is the same in time as the time history of eq. (3.8).

The vector displacement upon a point force in a unbounded domain is obtained in 3 steps:

- (i) Find body-force potentials Φ and Ψ such that

$\mathbf{f} = \dot{m}(t)\delta(\mathbf{x})\hat{\mathbf{x}} = \nabla\Phi + \nabla \times \Psi$ and $\nabla \cdot \Psi = 0$,
where $m(t)$ is the *source time function*,

- (ii) Solve wave equations for the potentials ϕ and ψ ,

- (iii) Form $\nabla\phi + \nabla \times \psi$.

Upon some pages of grungy algebra (see Aki & Richards, 2002, p.68-72), and using direction cosines $\gamma_i = x_i/r = \partial_r x_i$ such that $\partial_i \partial_j \frac{1}{r} = (3\gamma_i \gamma_j - \delta_{ij})/r^3$, we can write the solution in index notation as

$$u_i(\mathbf{x}, t) = \underbrace{\frac{3\gamma_i \gamma_j - \delta_{ij}}{4\pi\rho} \frac{1}{r^3} \int_{r/v_p}^{r/v_s} \tau \dot{m}(t - \tau) d\tau}_{\text{near-field term}} + \underbrace{\frac{\gamma_i \gamma_j}{4\pi\rho} \frac{1}{v_p^2 r} \dot{m} \left(t - \frac{r}{v_p} \right)}_{\text{far-field P-wave}} - \underbrace{\frac{\gamma_i \gamma_j - \delta_{ij}}{4\pi\rho} \frac{1}{v_s^2 r} \dot{m} \left(t - \frac{r}{v_s} \right)}_{\text{far-field S-wave}} \quad (3.10)$$

This is an important result that fully describes elastic wave propagation upon a force in the x_j direction in the absence of media variations and domain boundaries, and was first obtained by Stokes in 1849.

Far-field terms

If the excitation force is time-limited (i.e. goes back to zero after a period), the *far-field terms* are transient and \mathbf{u} is proportional to the rate of change of the source-time function $\dot{m}(t)$; no static displacement occurs. The amplitudes decay with $1/r$, i.e. slower than the near-field term.

More generally, the far-field compressional-wave displacement upon a moment-tensor source at $r = 0$ in polar coordinates (r, θ, ϕ) takes the form (Aki and Richards, 2002)

$$u_r = \frac{1}{4\pi\rho v_p^3 r} \dot{m}(t - r/v_p) \sin 2\theta \cos \phi. \quad (3.11)$$

The first term is an amplitude, note the cubic dependence on the velocity, and decays inversely linear with distance. The second term represents a temporal pulse propagating at speed v_p , i.e. the *source time function*. The trigonometric terms describe the radiation pattern, in this case 4 lobes with each 2 positive and negative lobes. Conversely, the shear-wave displacements perpendicular to u_r become

$$u_\theta = \frac{1}{4\pi\rho v_s^3 r} \dot{m}(t - r/v_s) \cos 2\theta \cos \phi, \text{ and} \quad (3.12)$$

$$u_\phi = \frac{1}{4\pi\rho v_s^3 r} \dot{m}(t - r/v_s) (-\cos \theta \sin \phi). \quad (3.13)$$

This S -wave motion does not have nodal planes, and thus does not reflect the fault geometry as clearly as P -waves. It is noteworthy to examine the average amplitudes between P and S waves which depends on $(v_p/v_s)^3 \approx 5$, suggesting that S waves typically have much larger amplitudes than P waves.

We will now turn to each of these terms separately. The following important properties hold:

P -wave far-field terms:	S -wave far-field terms:
<ul style="list-style-type: none"> attenuates as r^{-1}, propagates with wavespeed v_p and arrives at r/v_p, has displacement waveform proportional to the applied force at retarded time, has direction of displacement <i>parallel</i> to direction γ from the source, i.e. <i>longitudinal</i>. 	<ul style="list-style-type: none"> attenuates as r^{-1}, propagates with wavespeed v_s and arrives at r/v_s, has displacement waveform proportional to the applied force at retarded time, has direction of displacement <i>perpendicular</i> to direction γ from the source, i.e. <i>transverse</i>.

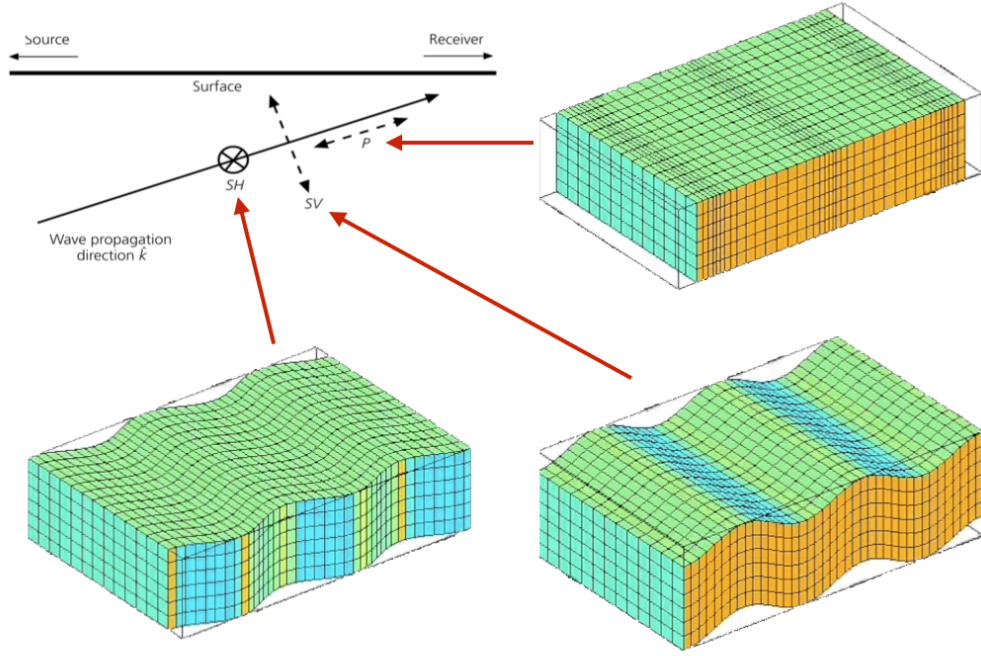


Figure 1: *Polarization with respect to the direction of elastic wave propagation for P-waves (top right), SH-waves (bottom left), and SV-waves (bottom right).*

Near-field terms

For short excitation $\dot{m}(t)$ compared to $r/v_s - r/v_p$, the first term is proportional to r^{-2} , and decays more rapidly than the far-field terms. Being proportional to $\dot{m}(t)$, static displacement remains (e.g. visible as surface-rupture of large earthquakes is a *near-field effect*). This term contains contributions from both the gradient of the scalar potential and from the curl of the vector potential, and consequently a mixture of *P*- (longitudinal) and *S*-wave (transverse) motion. This term only vanishes if the source-time function is finite: If there is permanent slip, it is manifested in an indefinite near-field displacement. The near-field only plays a role in near-source studies such as earthquake engineering.

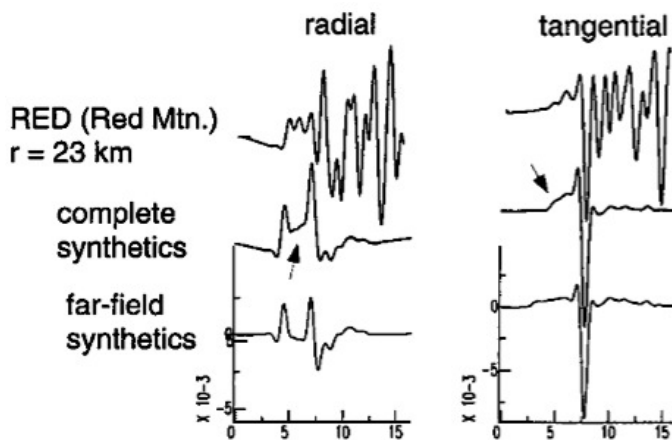


Figure 2: *Figure from Ichinose et al., 2000. The arrows point to motion that is attributed to the near-field term, as it cannot be replicated by far-field solutions. The earthquake was a $M_w=4.0$ in Calico Hills (California), recorded at $r=23\text{km}$.*

In the context of global seismology, we will mainly rely on the *far-field approximation*. This is valid for $r \gg L$ and $r \gg \lambda$, where L is some characteristic source dimension and λ the wavelength under consideration. This can also be expressed in terms of frequency: $|\omega| \gg v_{s/p}/r$ or $|\omega|T_r \ll 1$ and $r \gg \lambda$, (T_r : total rupture duration).

Excuse: Double-couple solutions

What we have discussed thus far is the wavefield solution due to a single-force excitation. For *double-couple sources* described by the second-order moment tensor \mathbf{M} , the expressions change slightly as we need to use Green function derivatives.

For the far-field P -wave Green's function, the partial derivatives with respect to the different coordinates are truncated to omit higher-order terms. After some even funkier algebra, this leads to the solution

$$u_n(\mathbf{x}, t) = M_{pq} * G_{np,q} = \frac{1}{r^4} \left(\frac{15\gamma_n\gamma_p\gamma_q - 3\gamma_n\delta_{pq} - 3\gamma_p\delta_{nq} - 3\gamma_q\delta_{np}}{4\pi\rho} \right) \int_{r/v_p}^{r/v_s} \tau M_{pq}(t - \tau) d\tau + \\ \frac{1}{r^2} \left(\frac{6\gamma_n\gamma_p\gamma_q - \gamma_n\delta_{pq} - \gamma_p\delta_{nq} - \gamma_q\delta_{np}}{4\pi\rho v_p^2} \right) M_{pq} \left(t - \frac{r}{v_p} \right) - \\ \frac{1}{r^2} \left(\frac{6\gamma_n\gamma_p\gamma_q - \gamma_n\delta_{pq} - \gamma_p\delta_{nq} - 2\gamma_q\delta_{np}}{4\pi\rho v_s^2} \right) M_{pq} \left(t - \frac{r}{v_s} \right) + \\ \frac{1}{r} \left[\frac{\gamma_n\gamma_p\gamma_q}{4\pi\rho v_p^3} \dot{M}_{pq} \left(t - \frac{r}{v_p} \right) - \frac{\gamma_n\gamma_p\gamma_q - \delta_{np}}{4\pi\rho v_s^3} \gamma_q \dot{M}_{pq} \left(t - \frac{r}{v_s} \right) \right] \quad (3.14)$$

The radiated displacement field due to a general 2nd-order moment tensor contains near-field terms, proportional to $r^{-4} \int \tau \mathbf{M}$, intermediate terms proportional to $r^{-2} \mathbf{M}$ and the far-field displacements that are proportional to $\frac{1}{r} \dot{\mathbf{M}}$.

Intermediate-field is a misnomer as there is no validity region for this, such that they are typically considered together with the near-field terms. Recall that the components of the moment tensor \mathbf{M} are proportional to particle displacements averaged over a fault plane (if the fault dimension is small compared to the wavelength), such that \dot{M}_{pq} , giving the pulse shape in the far fields, are proportional to particle *velocities* over the averaged fault plane.

Analytical solution to Lamb's Problem: Free surface and halfspace

We now introduce a boundary to the domain as the next complexity. *Lamb's Problem* consists of an impulsive vertical single force on a free surface above a homogeneous halfspace. In the interest of time, we simply showcase the mathematical complexity of such an allegedly simple problem, zooming into p. 35 of the classic paper by Lamb (1904) "On the propagation of tremors over the surface of an elastic solid".

TREMORS OVER THE SURFACE OF AN ELASTIC SOLID.

35

$$\begin{aligned} \mathfrak{P} \int_{-\infty}^{\infty} \frac{k^2 \xi \alpha}{F(\xi)} e^{ik\varpi \cosh u} d\xi &= 2\pi\kappa K \sin(\kappa\varpi \cosh u) - 2k^2 \mathfrak{P} \int_k^{\infty} \frac{\xi \alpha}{F(\xi)} e^{-ik\varpi \cosh u} d\xi \\ &\quad - 2k^2 \int_k^{\infty} \frac{\xi(2\xi^2 - k^2)^2 \alpha}{F(\xi) f(\xi)} e^{-ik\varpi \cosh u} d\xi. \end{aligned} \quad (151),$$

where H and K are the numerical quantities defined by (68) and (71). Substituting in (149) we have

$$\mathfrak{P}q_0 = -\frac{\kappa R}{2\mu} \cdot H \cdot K_1(\kappa\varpi) + \frac{ik^2 R}{\pi\mu} \int_k^{\infty} \frac{\xi^2(2\xi^2 - k^2)\alpha\beta}{F(\xi) f(\xi)} D_1(\xi\varpi) d\xi. \quad (152),$$

$$\begin{aligned} \mathfrak{P}w_0 &= \frac{i\kappa R}{2\mu} \cdot K \cdot J_0(\kappa\varpi) - \frac{ik^2 R}{2\pi\mu} \mathfrak{P} \int_k^{\infty} \frac{\xi \alpha}{F(\xi)} D_0(\xi\varpi) d\xi \\ &\quad - \frac{ik^2 R}{2\pi\mu} \int_k^{\infty} \frac{\xi(2\xi^2 - k^2)^2 \alpha}{F(\xi) f(\xi)} D_0(\xi\varpi) d\xi. \end{aligned} \quad (153),$$

where the notation of the various BESSEL'S Functions is as in Art. 2.

Superposing the system of free waves in which

$$q_0 = \frac{i\kappa R}{2\mu} \cdot H \cdot J_1(\kappa\varpi), \quad w_0 = -\frac{i\kappa R}{2\mu} \cdot K \cdot J_0(\kappa\varpi). \quad (154),$$

we obtain, finally, on inserting the time-factor,

$$q_0 = -\frac{\kappa R}{2\mu} \cdot H \cdot D_1(\kappa\varpi) e^{ip\ell} + \frac{ik^2 R}{\pi\mu} \int_k^{\infty} \frac{\xi^2(2\xi^2 - k^2)\alpha\beta}{F(\xi) f(\xi)} D_1(\xi\varpi) e^{ip\ell} d\xi. \quad (155),$$

$$w_0 = -\frac{ik^2 R}{2\pi\mu} \mathfrak{P} \int_k^{\infty} \frac{\xi \alpha}{F(\xi)} D_0(\xi\varpi) e^{ip\ell} d\xi - \frac{ik^2 R}{2\pi\mu} \int_k^{\infty} \frac{\xi(2\xi^2 - k^2)^2 \alpha}{F(\xi) f(\xi)} D_0(\xi\varpi) e^{ip\ell} d\xi. \quad (156).$$

Since these expressions are made up entirely of diverging waves, they constitute the complete solution of the problem where a periodic normal force $Re^{ip\ell}$ is applied to the surface at the origin.

Figure 3: Excerpt from Horace Lamb's paper in 1904, the solution to an impulsive force on a free surface above a halfspace. This paper contains the first synthetic seismogram ever computed.

The solution is built upon spherical Bessel functions, Weyl integrals (superposition of plane waves), Sommerfeld integrals (superposition of conical waves). A popular method to solve such systems is via the Cagniard-de Hoop method which evaluates multidimensional Laplace transforms.

Short note

As demonstrated by the complexity of Lamb's Problem, we will not proceed with full analytical solutions within this course, but instead turn to linking body waves to previous solutions, before approximating the physics for complex media and geometries.

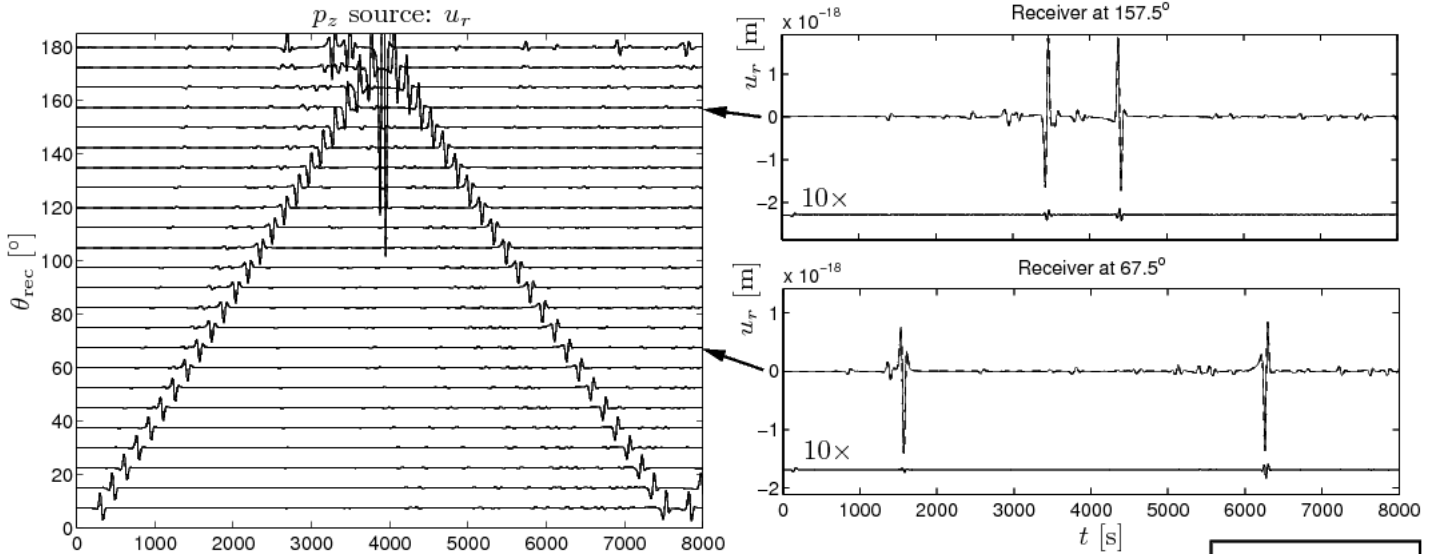


Figure 4: *Lamb's Problem solved with two methods: Numerical (spectral-element method) and quasi-analytical (normal mode summation) in a spherical, homogeneous, elastic Earth (taken from Tarje Nissen-Meyer's dissertation, 2007).*

3.3 Body wave propagation

Before we can define a nomenclature for traveling paths of different seismic body wave signals, we briefly have to introduce the concept of seismic rays. Note, the different solutions to the momentum equation in terms of normal modes, surface waves and body waves have many equivalent features; in this section we sketch some of the connections.

Generally, earthquakes produce compressional and shear motion, where shear motion is usually further subdivided into two types regarding the particle motion, to result in three types for the 3-vectorial displacement. *Transverse shear motion* is manifested in *SH*-waves, toroidal excitation, and Love waves. Shear motion with *longitudinal polarization* is seen in *SV*-waves, spheroidal excitation, and Rayleigh waves. *Compressional motion* is exclusive to *P*-waves, spheroidal and radial excitation, and Rayleigh waves. Since transverse/toroidal motion is orthogonal to *P – SV*-type motion and purely due to shear, it is impossible to transfer any such energy into compressional motion through conversions. Hence, horizontally polarized *SH* motion is the easiest conceptually and mathematically. In the following section we will largely depict the dualities for such toroidal motion.

Physical approximations

If we want to turn to more complex settings than a homogeneous halfspace, we require approximations to the momentum equation, and even though numerical techniques have been proposed for decades, non-numerical methods are widely utilized due to limitations in computational power.

We distinguish three types of approximations:

- (i) **Physics:** Acoustic instead of anisotropic, (an-)elastic equations of motion,
- (ii) **Dimension:** Collapse the wave equation into a 1D, 2D, or 2.5D domain,
- (iii) **Frequency:** Infinite-frequency assumption leading to ray theory.

In small-scale settings (e.g. exploration industry), one often assumes acoustic media in a cartesian, unbounded domain, i.e. wave propagation through an endless fluid, possibly 2D. In the global context, we will mainly instead follow the third simplification: *ray theory*. Much alike electromagnetic waves versus optical rays, seismic energy can be seen as propagating in infinitesimally thin, geometrical rays rather than full wavefields. This can be seen as an infinite-frequency approach ($\lambda \gg L$ where L is a typical scale length of structure).

Figure 3.7-8: Different approaches to wave propagation in a heterogeneous medium.

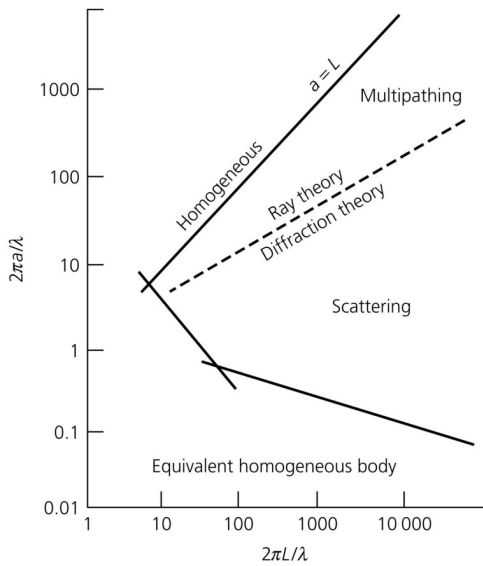


Figure 5: Representation of different approaches to seismic wave propagation in heterogeneous settings. The crucial distinction is the ratio of heterogeneity size a to wavelength λ and the propagation distance L .

In the following, we shall focus on the implications, advantages, and limitations of using ray theory in global seismology.

Ray-theory primer

Seismic rays in a spherically symmetric Earth are confined to the source-receiver great-circle plane. Let v be the wavespeed (P or S), and i the angle of incidence between a ray and the local upward vertical. The unit slowness vector is $\hat{\mathbf{p}} = \hat{\mathbf{r}} \cos i + \hat{\boldsymbol{\theta}} \sin i$. v, i, r all vary along the ray, however the *ray parameter* $p = (r \sin i)/v$ does not change.

Benndorf's relation links the ray parameter to the travel time T and angular distance Θ as: $p = dT/d\Theta$.

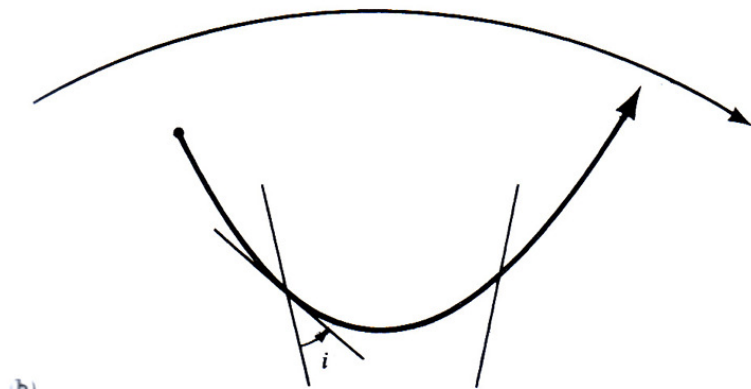


Figure 6: Seismic ray in a spherical earth with depth-dependent wavespeeds $v(r)$. i is the incidence angle.

Excursion: Mode-ray duality

Free oscillations are standing waves produced by constructive interference of propagating SH and $P - SV$ body waves that all have the same ray parameter, i.e. turn at the same radius. The spherical surface with this radius R is an envelope of rays, or a *caustic*. The task to find the modes of the Earth is fundamentally a quantization problem: requirement for constructive interference is an integral number of oscillations to fit onto the surface of the sphere and between two radii $r = R$ and $r = R_{\text{Earth}}$, analogous to the Bohr-Sommerfeld quantization in quantum mechanics. The angular quantization is characterized by the total phase accumulated in a single complete passage of a wave around the Earth $\Delta\Psi = -2\pi\omega p + \pi$ where the latter term reflects a $\pi/2$ phase shift upon passing through a caustic. The Bohr-Sommerfeld condition for constructive interference is $|\Delta\Psi| = 2\pi l$ (l : non-negative integer). This yields the *Jeans relation*

$$\omega p = l + \frac{1}{2}. \quad (3.15)$$

The quantum number l is the angular degree of the normal modes ${}_nT_l$.

Ray theory & the eikonal equation

Definition. For a given wavefront $S = \omega/k_0 t - \epsilon/k_0$, rays \mathbf{x} are the normals to S as the wavefront propagates, and represent fixed curves in space. We parameterize rays $\mathbf{x} = \mathbf{x}(\xi)$ with ξ changing monotonically along the ray. Then $d\mathbf{x}/d\xi = g(\mathbf{x})\nabla T$ describes a ray equation where $g(\mathbf{x})$ is a scalar function relating parallel vectors. For example, choosing

$$\frac{d\mathbf{x}}{d\xi} = c^2 \nabla T = (c \nabla T) c \quad (3.16)$$

means that ξ is interpreted as a *travel time*, and $c \nabla T$ is the unit normal to S propagating at speed c . Then,

$$\frac{dT}{d\xi} = \nabla T \cdot \frac{d\mathbf{x}}{d\xi} = 1 \quad \text{and} \quad \frac{d\mathbf{x}}{ds} = c \nabla T. \quad (3.17)$$

Waves at interfaces

Fermat's Principle governs the geometry of a ray such that it follows an minimal-time path. Snell's Law, relating incidence and transmitted angle to velocities on either side of a discontinuity, is a direct consequence, and reads in spherical geometry

$$\frac{r_1 \sin i_1}{v_1} = \frac{r_1 \sin i'_1}{v_2} = \frac{r_2 \sin i_2}{v_2} \quad (3.18)$$

since $r_1 \sin i'_1 = r_2 \sin i_2$. The ray parameter as defined above ($p = r/v \sin i$) reinstates the fact that it identifies an entire ray, irrespective of its reflections, transmissions, and refractions along the path.

We will now analyze the reflection and transmission properties for seismic waves, but revert to a cartesian setting for simplicity of notation, assuming a piecewise constant velocity profile with parallel layers of distinct velocity jumps. The incidence angle onto a horizontal boundary is $i_2 = \sin^{-1} [i_1(\alpha_2/\alpha_1)]$, implying that the transmitted wave into a larger velocity medium is further from the vertical than the incident wave. As the incident angle increases, the transmitted ray approximates the horizontal, eventually reaching the *critical angle*:

$$i_c = \sin^{-1} (\alpha_1 \alpha_2) \quad (3.19)$$

Once this critical angle is exceeded, one speaks of the postcritical regime in which no energy is transmitted, also known as *total internal reflection*. The P -wave potential in the second layer has a real exponential dependence in z rather than an imaginary one, and hence decays exponentially with depth, also known as *evanescent wave*.

Let's have a brief look at **reflection and transmission properties**, focusing for ease of notation on SH waves. This is done by a plane-wave Ansatz, making use of solid-solid interface conditions, stating that displacement and traction are continuous across the interface $z = 0$. We have in the upper (2D) medium a downgoing and reflected component of the wavefield ($r_\beta = k_{z\beta}/k_x = \cot j$, ratio of vertical to horizontal wavenumber):

$$u_y^-(x, z, t) = B_1 \exp(i(\omega t - k_x x - k_x r_{\beta_1} z)) + B_2 \exp(i(\omega t - k_x x + k_x r_{\beta_1} z)), \quad (3.20)$$

and in the lower medium ($z > 0$) a transmitted wave

$$u_y^+(x, z, t) = B' \exp(i(\omega t - k_x x - k_x r_{\beta_2} z)). \quad (3.21)$$

Displacement continuity requires

$$(B_1 + B_2) \exp(i(\omega t - k_x x) = B' \exp(i(\omega t - k_x x)). \quad (3.22)$$

Upon canceling the exponents with $\omega t - k_x x$, we find $B_1 + B_2 = B'$. Traction continuity for SH waves means that $\sigma_{yz}^-(x, 0, t) = \sigma_{yz}^+(x, 0, t)$. Inserting this into Hooke's Law and the plane wave Ansatz, canceling factors on both sides we obtain $(B_1 - B_2) = B'(\mu_2 r_{\beta_2})/(\mu_1 r_{\beta_1})$. Putting these two conditions together, we eliminate B_2 to find the transmission coefficient

$$T_{12} = \frac{B'}{B_1} = \frac{2\rho_1 \beta_1 \cos j_1}{\rho_1 \beta_1 \cos j_1 + \rho_2 \beta_2 \cos j_2}, \quad (3.23)$$

and eliminating B' to find the reflection coefficient

$$R_{12} = \frac{B_2}{B_1} = \frac{\rho_1 \beta_1 \cos j_1 - \rho_2 \beta_2 \cos j_2}{\rho_1 \beta_1 \cos j_1 + \rho_2 \beta_2 \cos j_2}, \quad (3.24)$$

where we have used $r_{\beta_i} = c_x \cos j_i / \beta_i$.

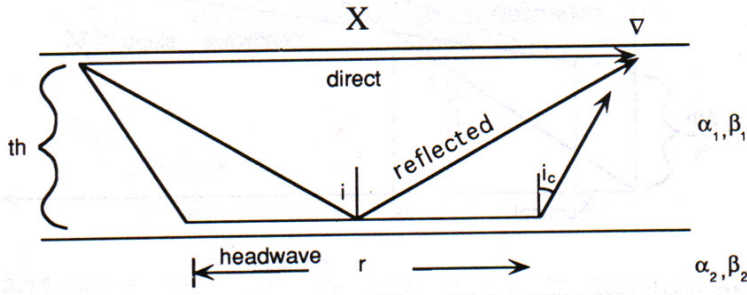


Figure 7: Sketch to identify crucial parameters in a setting of direct, reflected, diffracted waves upon one discontinuity.

The basic idea to obtain earth models is to analyze arrival times in terms of velocity structure. Let us look at a simple geometrical problem of finding the arrival times of the respective rays as in Fig. 7, given by

$$T_{\text{refl.}} = \frac{2d}{\alpha_1 \cos i}; \quad T_{\text{refr.}} = \frac{2d}{\alpha_1 \cos i} + \frac{r}{\alpha_2}, \quad (3.25)$$

where $r = X - 2d \tan i_c$. Using Snell's Law, we can rewrite the refracted arrival time as

$$T_{\text{refr.}} = \frac{2d}{\alpha_1 \cos i_c} + \frac{1}{\alpha_2} \left(X - \frac{2d\alpha_1}{\alpha_2 \cos i_c} \right), \quad (3.26)$$

and using $\alpha_1^{-1} = p$, $\cos i_c = \sqrt{1 - p^2 \alpha_1^2} = \eta_1$, we obtain

$$T_{\text{refr.}} = Xp + \sum_i 2d_i \eta_i, \quad (3.27)$$

where we generalized into a sum of multiple layers. This expression conveniently separates the arrival time into a vertical and horizontal term and naturally generalizes to a continuous medium, i.e. infinite number of layers. A *low-velocity layer* leads to observing only a refracted wave from the lower half space, possibly misinterpreted as a 2-layer model and an overestimation of the depth of the last layer. A *blind zone* occurs if a layer is so thin that its head wave never becomes a first arrival.

Traveltime curves

Given a time-distance T-X diagram from some observations, we are now interested in the slope $dT/dX = 1/c$. At each point along a ray, we can write $\sin i = dx/ds = cp$, where c is the local velocity. Using $\cos i = \sqrt{1 - c^2 p^2}$, we obtain

$$dx = ds \sin i = \frac{dz}{\cos i} cp = \frac{cp}{\sqrt{1 - c^2 p^2}} dz, \quad (3.28)$$

and integrate to arrive at

$$X = 2 \int_0^z \frac{cp}{\sqrt{1 - c^2 p^2}} dz, \quad (3.29)$$

which predicts the epicentral distance given p (or emergence angle) and velocity structure. The corresponding travel time is

$$T = 2 \int_0^z \frac{dz}{c^2 \sqrt{1/c^2 - p^2}} = pX + 2 \int_0^z \sqrt{1/c^2(z) - p^2} dz, \quad (3.30)$$

similar to the form of the refracted traveltimes. The traveltime curve is then given by

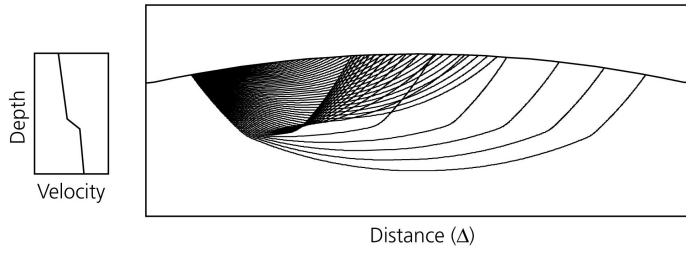
$$\tau(p) = T - pX = 2 \int_0^p \sqrt{1/c^2(z) - p^2} dz, \quad (3.31)$$

and the *intercept time* at $X = 0$ is

$$\frac{d\tau}{dp} = 2 \int_0^z \frac{-p}{\sqrt{1/c^2(z) - p^2}} dz = -X. \quad (3.32)$$

This single-valued function is easier to analyze than the sometimes multi-valued travel time.

Ray path triplication effects for a velocity increase.



Ray path shadow-zone effects for a velocity decrease.

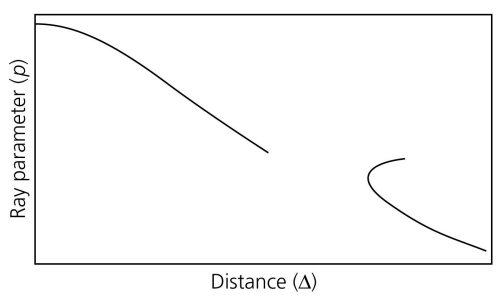
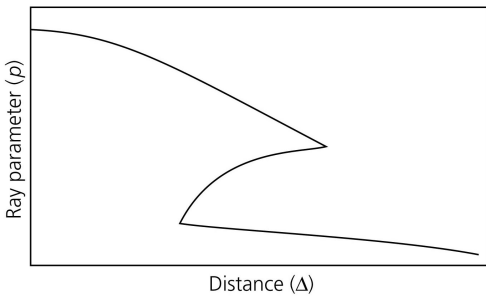
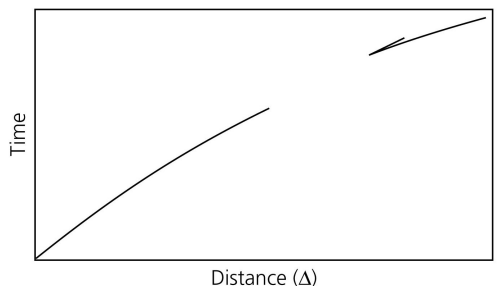
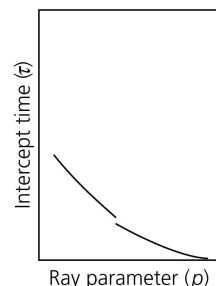
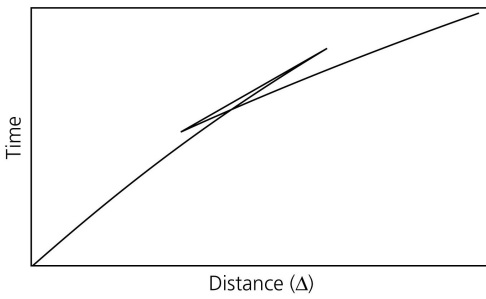
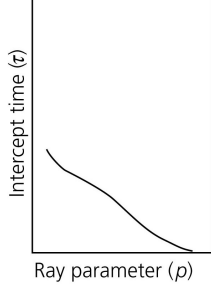
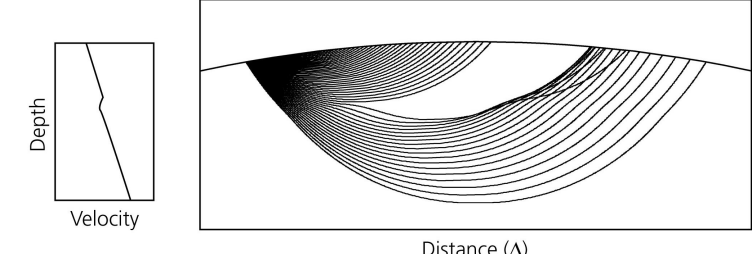


Figure 8: *Left: Triplication. Such a point in the time-distance plot occurs at points where three phases arrive at the same time, i.e. the three branches in the ray parameter plot. This occurs with rapid velocity increases such that the transmitted phase eventually arrives earlier than the phase in the upper layer. Right: Shadow Zone. Such a gap in the time-distance plot hints at a layer with lower velocities than the layer above.*

The above results can be rewritten in analogous form for the spherical case as

$$T = p\Delta + 2 \int_{r_0}^{r_1} \frac{r^2/c^2(z) - p^2}{r^2} dr, \quad (3.33)$$

where equivalently the second term only depends on the radial direction.

Figure 3.4-1: Geometry of Snell's law for a spherical earth.

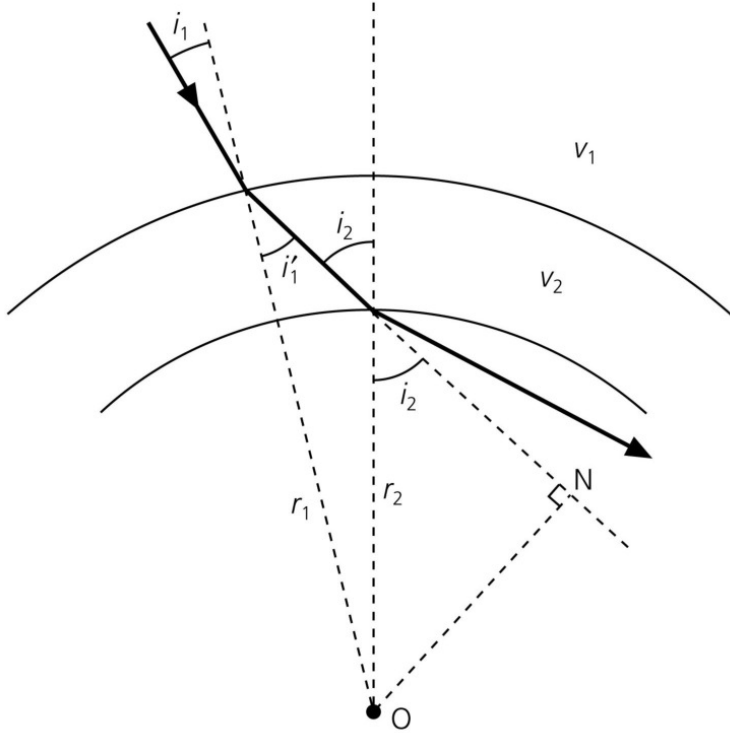


Figure 9: *Geometry of Snell's Law of reflection in a spherical Earth.*

Wiechert-Herglotz Method: Inversion for structure

The last section constitutes the forward solution to travel times. We are now interested in using this to determine the structure of the Earth, i.e. solve an inverse problem of the form $\sum_{\text{traveltimes}} (T_{\text{obs}} - T_{\text{theory}}(m)) = \min$. Starting with

$$X(p) = 2 \int_0^{Z(p)} \frac{p}{\sqrt{c(z)^{-2} - p^2}} dz, \quad (3.34)$$

after some algebraic manipulations, this turns out as

$$z(c) = -\frac{1}{\pi} \int_{c_0^{-1}}^{c^{-1}} \frac{X(p)}{\sqrt{p^2 - c^{-2}}} dp, \quad (3.35)$$

which is an analytical solution for the case of no low-velocity channels, but allows for rapid velocity increases and discontinuous derivatives of $X(p)$.

3.4 Seismic phases, traveltimes & Earth structure

Seismic phases are pulses on a seismogram that are traced back to a specific ray path associated with a wave type (e.g. reflected, P-to-S conversion). *Traveltimes* are scatter plots of “picked” traveltimes as a function of epicentral distance, upon which one usually labels seismic phases.

To obtain a model for Earth structure, one needs to “invert” the system $\mathbf{d} = f(\mathbf{m})$ where \mathbf{d} is a data vector, \mathbf{m} an Earth model, and f the generic function that relates the two, i.e. in seismology some version of the momentum equation. The inverse operation is generally non-linear, and solutions are much more varied and ill-posed, not to mention unverifiable compared to the forward problem treated so far in this course. We shall simply mention some methods used to obtain Earth models since these form the basis for any realistic forward solutions, but advise you to gather any more in-depth treatment in courses on inverse theory and tomography.

Figure 3.5-2: Selection of body phases and their ray paths.

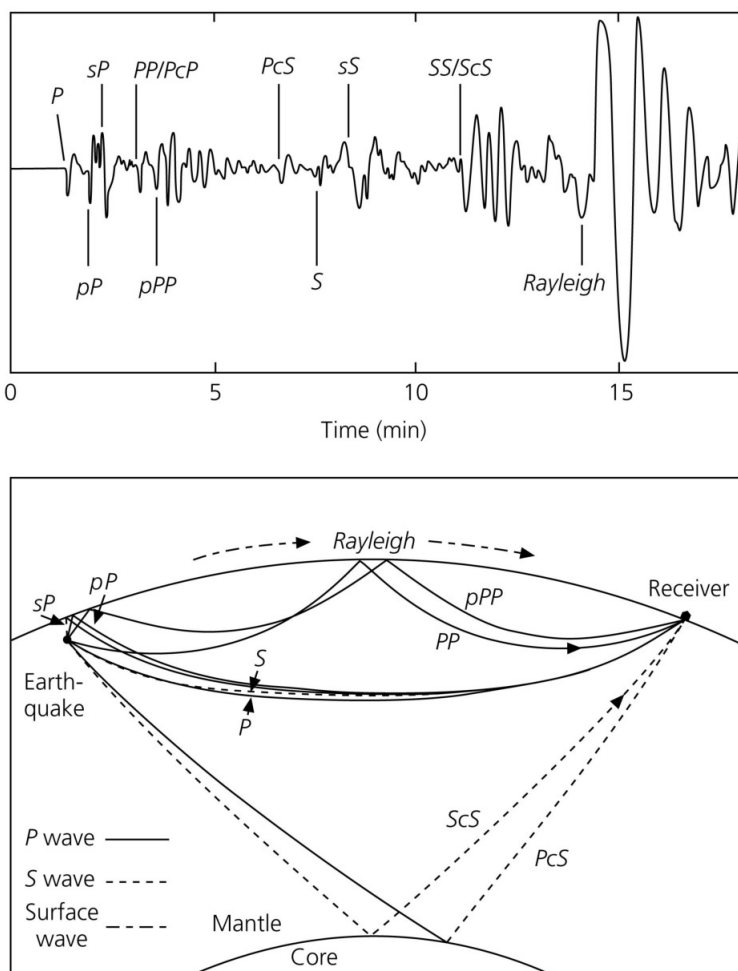


Figure 10: Long-period vertical component seismogram (top), and ray paths for some of the phases. Note that P and S phases travel different paths since their velocities (and hence behavior due to Snell’s Law) differ; for instance the path of PcS is asymmetric.

Phase nomenclature and picking

Seismic phases are denoted based on a (somewhat) consistent nomenclature:

P : compressional waves

PP : surface multiple (surface-reflected P wave)

S : shear waves

p : depth phases (upgoing from focus & reflected)

c : reflection from core-mantle boundary

K : wave inside core

i : Reflection from inner-core boundary

I : wave through inner core

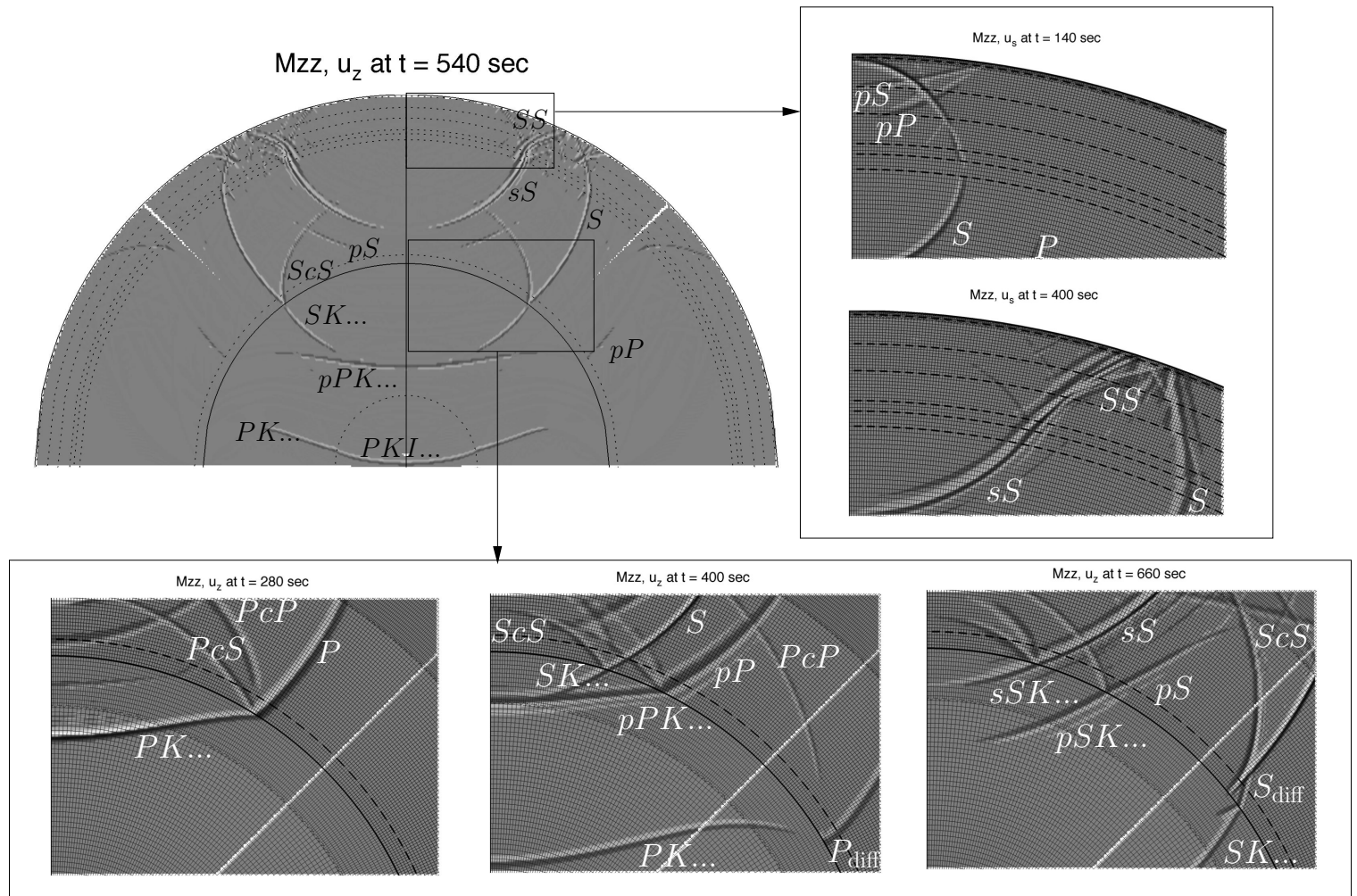


Figure 11: Snapshot of a numerical simulation of global waves for a PREM 1D Earth model, showcasing various prominent phases (Nissen-Meyer, 2007).

Traveltime curves & caustics

Figure 3.5-3: Travel time data and curves for the IASP91 model.

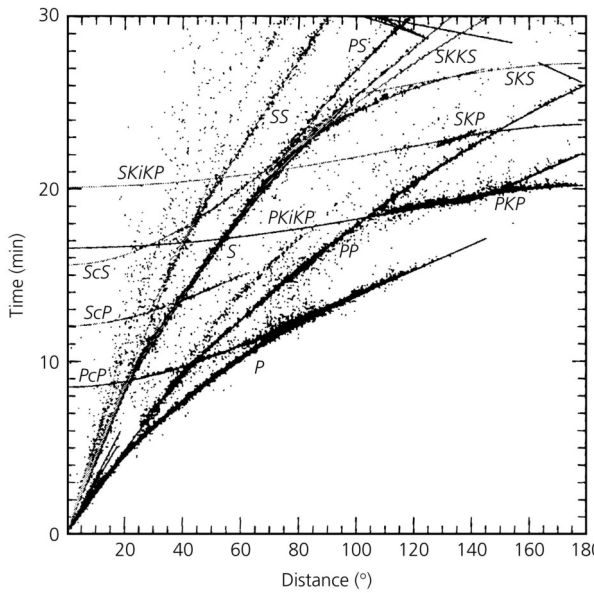
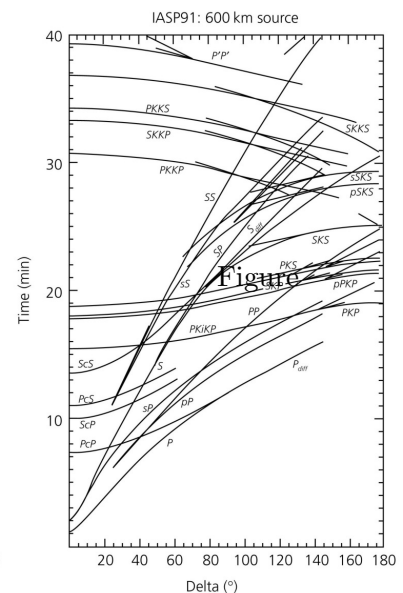
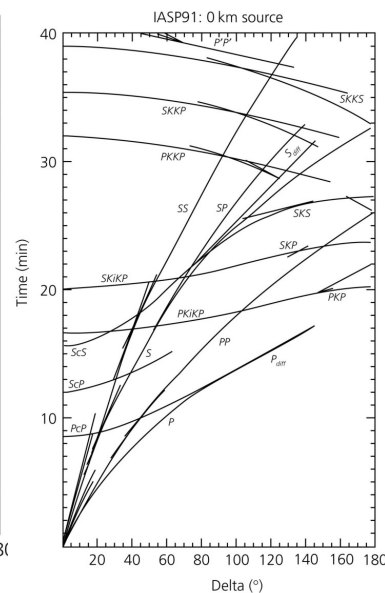


Figure 3.5-4: IASP91 travel time curves for a surface and deep source.



12: Left: 57,655 traveltime picks from 104 sources and curves upon model IASP91. Right: Traveltime curves for model IASP91 for two source depths.

Figure 3.5-7: Ray paths and travel times for major core phases.

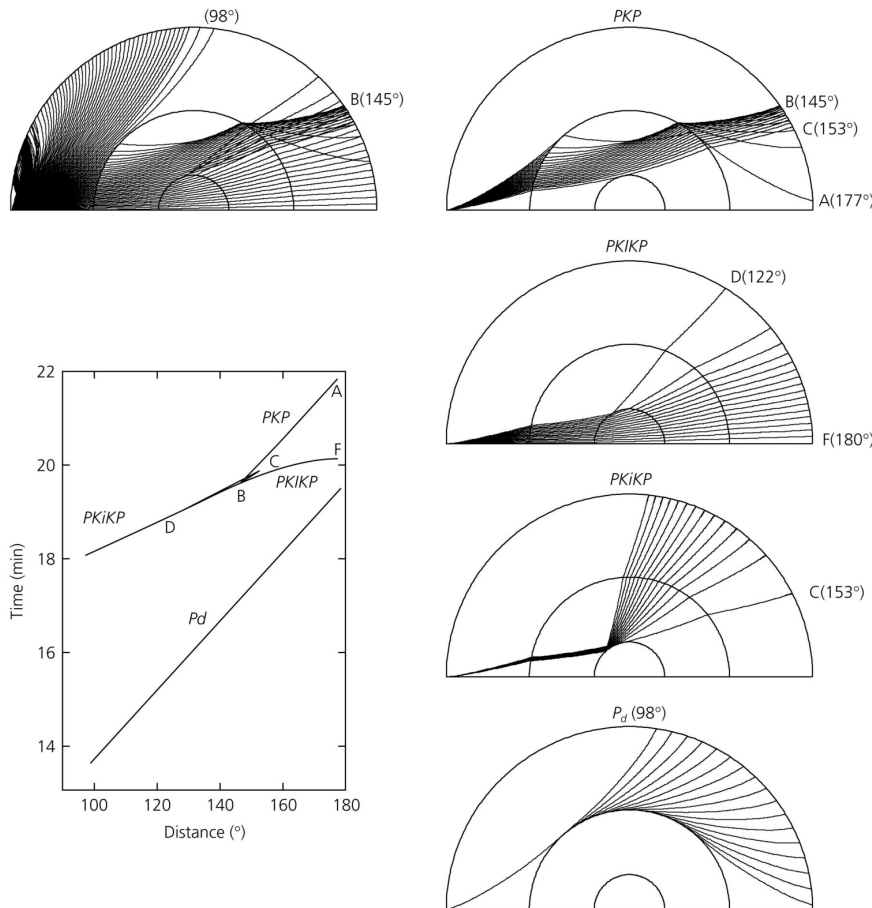


Figure 13: *Ray paths and traveltimes for major core phases (upon PREM).*

*Top left: Direct phases.
Right: reflected and
diffracted core phases.
Diffracted P (bottom)
is a pure wave phe-
nomenon and does not
appear in solutions
based on ray theory,
but is a well-defined,
observed pulse in real
seismograms.*

Spherically symmetric Earth models

The large-scale structure of the Earth has traditionally been subdivided into concentric spherical shells to distinguish the major seismic velocity jumps caused by mineralogical phase changes and physical discontinuities which, at a certain range of resolutions, satisfies up to 90% of seismic data. Seismic investigations for such 1D structure have enjoyed a long tradition, and these models are still widely used as a reliable basis for the bulk properties of the Earth.

Figure 3.5-1: Comparison of the J-B and IASP91 earth models.

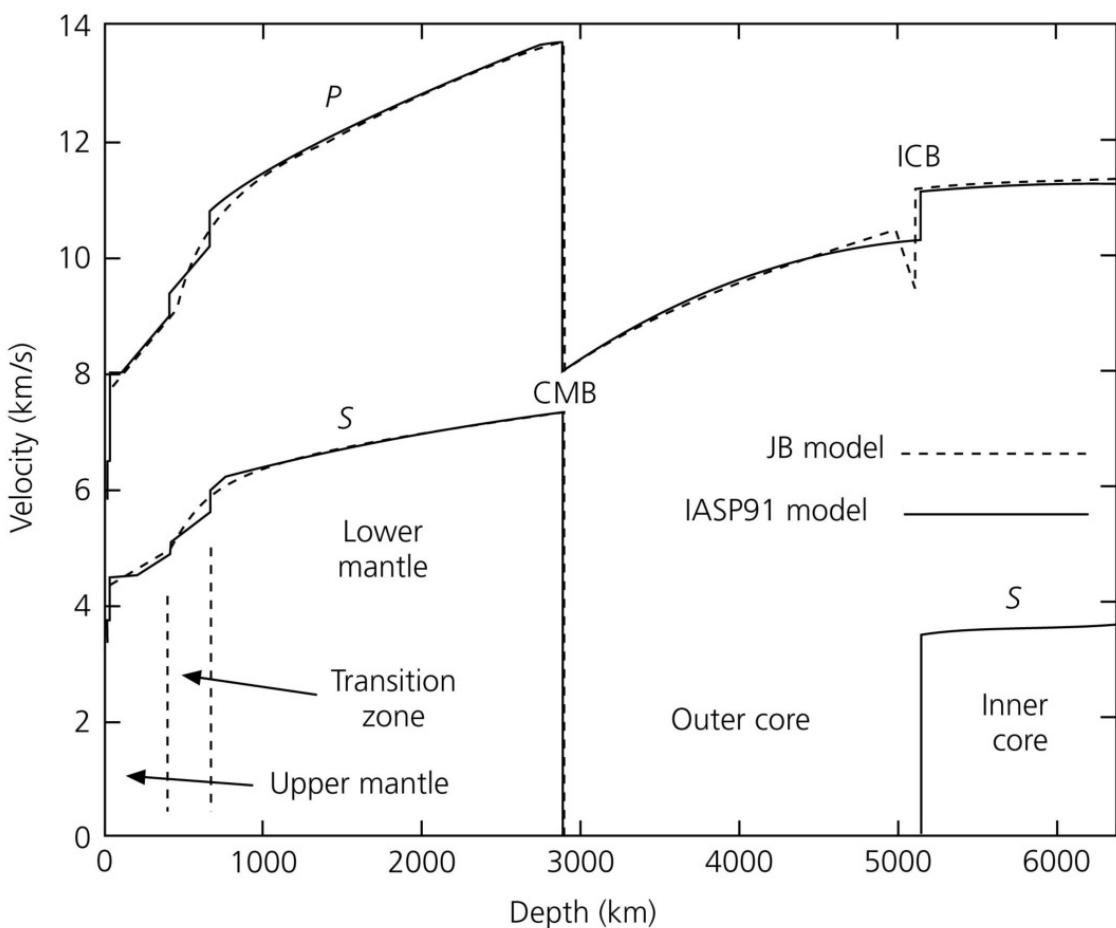


Figure 14: Comparison of the classic Jeffreys-Bullen earth model (1940) and IASP91 (Kennett & Engdahl, 1991). Although improved in mantle transition zone and core, the models differ very little despite the hand-cranked derivation of the former.

3D Earth models

Superimposed upon spherically symmetric Earth models are then *lateral heterogeneities* to represent the actual 3D structure and typically linked to the dynamic and tectonic state of the planet. These models are mostly obtained via tomographic inversions, and usually map perturbations much below 20% deviations from the 1D structure. In other words, geophysicists have a well-founded, acceptable account of 90% of the Earth's seismic properties, and almost all open debates center around the remaining 10%. This lies in curious diametrical opposition to astrophysics where bulk properties of the evolution of the universe are claimed upon understanding 10% of matter, ignoring 90% dark matter. We shall only touch upon 3D models which lie at the heart of modern geophysical research into understanding Earth's thermal, chemical, and tectonic state and evolution, and present fundamental input for geo-dynamics, mineral physics, geomagnetism, tectonics, and geochemistry.

Approximate (and computationally feasible) techniques to solve the momentum equation in 3D medium without reverting to fully discrete numerical techniques largely rely on ray theory. One example is the Gauss-Beam Method which improves results near caustics over classical ray methods, but WKBJ methods are still widely used in global tomography.

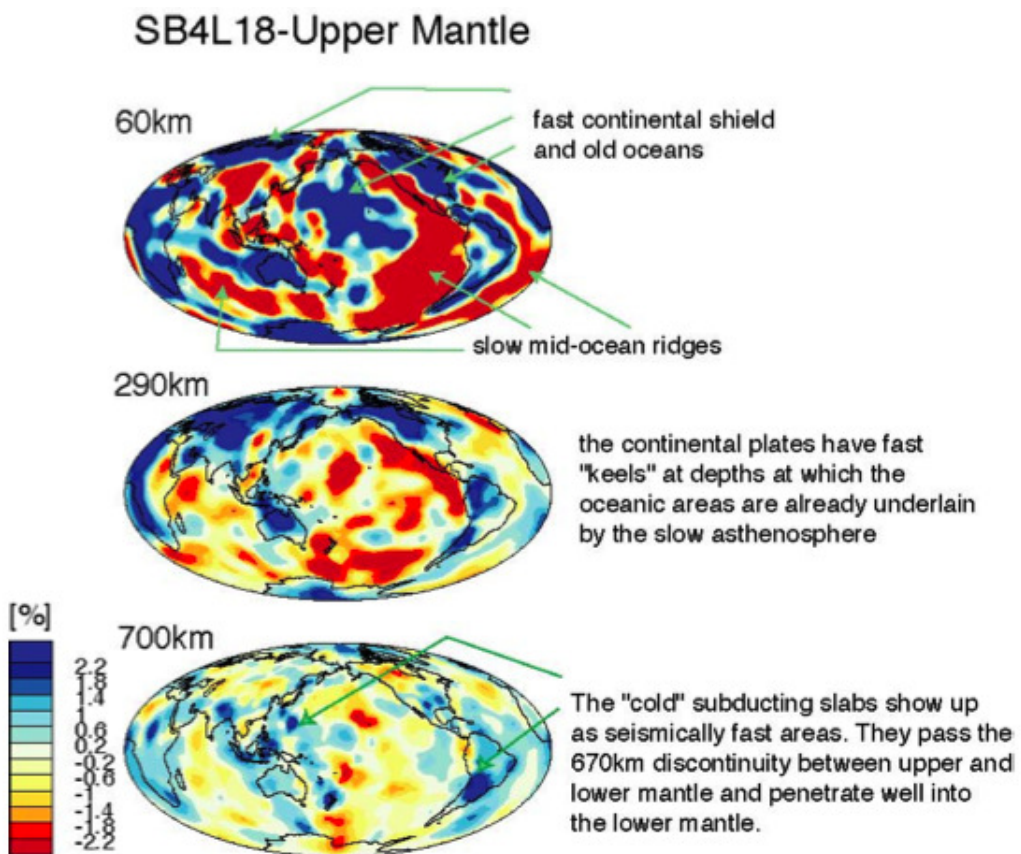


Figure 15: *Spherical shells from the 3D global tomography model SB4L18 throughout the upper mantle.*

Further reading

- Aki, K., and P. G. Richards, 2002. *Quantitative Seismology*, 2nd Edition, University Science Books: chapters 3, 10,11.
- Blakely, R. J., 1996. *Potential Theory in Gravity and Magnetic Applications*, 1st edition, Cambridge University Press.
- Dahlen, F. A., and J. Tromp, 1998. *Theoretical Global Seismology*, Princeton University Press.
- Ichinose, G., Goldstein, P., Rodgers, A., 2000. *Relative importance of Near-, Intermediate- and Far-Field displacement terms in layered earth synthetic seismograms*. Bull. Seis. Soc. Am., 90, 531-536.
- Lamb, H., 1904. *On the propagation of tremors over the surface of an elastic solid*, Phil. Trans. Roy. Soc. Lond., 203, 1-42.
- Stein, S. and M. Wysession, 2003. *An Introduction to Seismology, Earthquakes, and Earth Structure*, Blackwell Publishing, chapter 4.
- Other resources: Seismic travel time calculator TauP: <http://www.seis.sc.edu/taup>